



日本原子力研究開発機構機関リポジトリ
Japan Atomic Energy Agency Institutional Repository

Title	Measurement of time-dependent CP violation in $B^0 \rightarrow K_S^0 \pi^0 \pi^0$ decays
Author(s)	Yusa Yosuke, Tanida Kiyoshi, Belle Collaboration, 159 of others
Citation	Physical Review D,99(1),p.011102_1-011102_7
Text Version	Published Journal Article
URL	https://jopss.jaea.go.jp/search/servlet/search?5067896
DOI	https://doi.org/10.1103/PhysRevD.99.011102
Right	Published by the American Physical Society under the terms of the Creative Commons Attribution 4.0 International license. Further distribution of this work must maintain attribution to the author(s) and the published article's title, journal citation, and DOI. Funded by SCOAP ³ .

Measurement of time-dependent CP violation in $B^0 \rightarrow K_S^0 \pi^0 \pi^0$ decays

Y. Yusa,⁵⁹ H. Aihara,⁸⁰ S. Al Said,^{74,35} D. M. Asner,³ H. Atmacan,⁷¹ V. Aulchenko,^{4,60} T. Aushev,⁵⁰ R. Ayad,⁷⁴ V. Babu,⁷⁵ I. Badhrees,^{74,34} S. Bahinipati,²² A. M. Bakich,⁷³ V. Bansal,⁶² P. Behera,²⁵ V. Bhardwaj,²¹ B. Bhuyan,²³ J. Biswal,³² A. Bozek,⁵⁷ M. Bračko,^{44,32} T. E. Browder,¹⁶ L. Cao,³³ D. Červenkov,⁵ V. Chekelian,⁴⁵ A. Chen,⁵⁴ B. G. Cheon,¹⁵ K. Chilikin,⁴⁰ S.-K. Choi,¹⁴ Y. Choi,⁷² D. Cinabro,⁸⁴ S. Cunliffe,⁸ N. Dash,²² S. Di Carlo,³⁸ T. V. Dong,^{17,13} Z. Drásal,⁵ S. Eidelman,^{4,60,40} D. Epifanov,^{4,60} J. E. Fast,⁶² B. G. Fulsom,⁶² R. Garg,⁶³ V. Gaur,⁸³ A. Garmash,^{4,60} A. Giri,²⁴ P. Goldenzweig,³³ B. Golob,^{41,32} Y. Guan,^{26,17} J. Haba,^{17,13} K. Hayasaka,⁵⁹ H. Hayashii,⁵³ S. Hirose,⁵¹ K. Inami,⁵¹ G. Inguglia,⁸ A. Ishikawa,⁷⁸ R. Itoh,^{17,13} M. Iwasaki,⁶¹ Y. Iwasaki,¹⁷ W. W. Jacobs,²⁶ S. Jia,² Y. Jin,⁸⁰ K. K. Joo,⁶ K. H. Kang,³⁷ T. Kawasaki,⁵⁹ C. Kiesling,⁴⁵ D. Y. Kim,⁷⁰ J. B. Kim,³⁶ K. T. Kim,³⁶ S. H. Kim,¹⁵ K. Kinoshita,⁷ P. Kodyš,⁵ S. Korpar,^{44,32} D. Kotchetkov,¹⁶ P. Križan,^{41,32} R. Kroeger,⁴⁷ T. Kuhr,⁴² R. Kumar,⁶⁶ Y.-J. Kwon,⁸⁶ J. S. Lange,¹¹ I. S. Lee,¹⁵ S. C. Lee,³⁷ L. K. Li,²⁷ Y. B. Li,⁶⁴ L. Li Gioi,⁴⁵ J. Libby,²⁵ D. Liventsev,^{83,17} M. Lubej,³² T. Luo,¹⁰ M. Masuda,⁷⁹ T. Matsuda,⁴⁸ M. Merola,^{29,52} K. Miyabayashi,⁵³ H. Miyata,⁵⁹ R. Mizuk,^{40,49,50} G. B. Mohanty,⁷⁵ H. K. Moon,³⁶ E. Nakano,⁶¹ M. Nakao,^{17,13} T. Nanut,³² K. J. Nath,²³ Z. Natkaniec,⁵⁷ N. K. Nisar,⁶⁵ S. Nishida,^{17,13} K. Nishimura,¹⁶ K. Ogawa,⁵⁹ S. Ogawa,⁷⁷ H. Ono,^{58,59} G. Pakhlova,^{40,50} B. Pal,³ S. Pardi,²⁹ H. Park,³⁷ S. Paul,⁷⁶ T. K. Pedlar,⁴³ R. Pestotnik,³² L. E. Piilonen,⁸³ V. Popov,^{40,50} E. Prencipe,¹⁹ A. Rostomyan,⁸ G. Russo,²⁹ Y. Sakai,^{17,13} S. Sandilya,⁷ T. Sanuki,⁷⁸ V. Savinov,⁶⁵ O. Schneider,³⁹ G. Schnell,^{1,20} C. Schwanda,²⁸ A. J. Schwartz,⁷ Y. Seino,⁵⁹ K. Senyo,⁸⁵ O. Seon,⁵¹ M. E. Sevier,⁴⁶ C. P. Shen,² T.-A. Shibata,⁸¹ J.-G. Shiu,⁵⁶ M. Starić,³² M. Sumihama,¹² T. Sumiyoshi,⁸² M. Takizawa,^{69,18,67} U. Tamponi,³⁰ K. Tanida,³¹ F. Tenchini,⁴⁶ M. Uchida,⁸¹ T. Uglov,^{40,50} Y. Unno,¹⁵ S. Uno,^{17,13} Y. Ushiroda,^{17,13} Y. Usov,^{4,60} C. Van Hulse,¹ R. Van Tonder,³³ G. Varner,¹⁶ K. E. Varvell,⁷³ V. Vorobyev,^{4,60,40} A. Vossen,⁹ E. Waheed,⁴⁶ B. Wang,⁷ C. H. Wang,⁵⁵ M.-Z. Wang,⁵⁶ P. Wang,²⁷ E. Won,³⁶ H. Ye,⁸ J. H. Yin,²⁷ Z. P. Zhang,⁶⁸ V. Zhilich,^{4,60} and V. Zhulanov^{4,60}

(Belle Collaboration)

¹University of the Basque Country UPV/EHU, 48080 Bilbao²Beihang University, Beijing 100191³Brookhaven National Laboratory, Upton, New York 11973⁴Budker Institute of Nuclear Physics SB RAS, Novosibirsk 630090⁵Faculty of Mathematics and Physics, Charles University, 121 16 Prague⁶Chonnam National University, Kwangju 660-701⁷University of Cincinnati, Cincinnati, Ohio 45221⁸Deutsches Elektronen-Synchrotron, 22607 Hamburg⁹Duke University, Durham, North Carolina 27708¹⁰Key Laboratory of Nuclear Physics and Ion-Beam Application (MOE) and Institute of Modern Physics, Fudan University, Shanghai 200443¹¹Justus-Liebig-Universität Gießen, 35392 Gießen¹²Gifu University, Gifu 501-1193¹³SOKENDAI (The Graduate University for Advanced Studies), Hayama 240-0193¹⁴Gyeongsang National University, Chinju 660-701¹⁵Hanyang University, Seoul 133-791¹⁶University of Hawaii, Honolulu, Hawaii 96822¹⁷High Energy Accelerator Research Organization (KEK), Tsukuba 305-0801¹⁸J-PARC Branch, KEK Theory Center, High Energy Accelerator Research Organization (KEK), Tsukuba 305-0801¹⁹Forschungszentrum Jülich, 52425 Jülich²⁰IKERBASQUE, Basque Foundation for Science, 48013 Bilbao²¹Indian Institute of Science Education and Research Mohali, SAS Nagar, 140306²²Indian Institute of Technology Bhubaneswar, Satya Nagar 751007²³Indian Institute of Technology Guwahati, Assam 781039²⁴Indian Institute of Technology Hyderabad, Telangana 502285²⁵Indian Institute of Technology Madras, Chennai 600036²⁶Indiana University, Bloomington, Indiana 47408²⁷Institute of High Energy Physics, Chinese Academy of Sciences, Beijing 100049²⁸Institute of High Energy Physics, Vienna 1050²⁹INFN—Sezione di Napoli, 80126 Napoli

- ³⁰INFN—Sezione di Torino, 10125 Torino
- ³¹Advanced Science Research Center, Japan Atomic Energy Agency, Naka 319-1195
- ³²J. Stefan Institute, 1000 Ljubljana
- ³³Institut für Experimentelle Teilchenphysik, Karlsruher Institut für Technologie, 76131 Karlsruhe
- ³⁴King Abdulaziz City for Science and Technology, Riyadh 11442
- ³⁵Department of Physics, Faculty of Science, King Abdulaziz University, Jeddah 21589
- ³⁶Korea University, Seoul 136-713
- ³⁷Kyungpook National University, Daegu 702-701
- ³⁸LAL, University Paris-Sud, CNRS/IN2P3, Université Paris-Saclay, Orsay
- ³⁹École Polytechnique Fédérale de Lausanne (EPFL), Lausanne 1015
- ⁴⁰P.N. Lebedev Physical Institute of the Russian Academy of Sciences, Moscow 119991
- ⁴¹Faculty of Mathematics and Physics, University of Ljubljana, 1000 Ljubljana
- ⁴²Ludwig Maximilians University, 80539 Munich
- ⁴³Luther College, Decorah, Iowa 52101
- ⁴⁴University of Maribor, 2000 Maribor
- ⁴⁵Max-Planck-Institut für Physik, 80805 München
- ⁴⁶School of Physics, University of Melbourne, Victoria 3010
- ⁴⁷University of Mississippi, University, Mississippi 38677
- ⁴⁸University of Miyazaki, Miyazaki 889-2192
- ⁴⁹Moscow Physical Engineering Institute, Moscow 115409
- ⁵⁰Moscow Institute of Physics and Technology, Moscow Region 141700
- ⁵¹Graduate School of Science, Nagoya University, Nagoya 464-8602
- ⁵²Università di Napoli Federico II, 80055 Napoli
- ⁵³Nara Women's University, Nara 630-8506
- ⁵⁴National Central University, Chung-li 32054
- ⁵⁵National United University, Miao Li 36003
- ⁵⁶Department of Physics, National Taiwan University, Taipei 10617
- ⁵⁷H. Niewodniczanski Institute of Nuclear Physics, Krakow 31-342
- ⁵⁸Nippon Dental University, Niigata 951-8580
- ⁵⁹Niigata University, Niigata 950-2181
- ⁶⁰Novosibirsk State University, Novosibirsk 630090
- ⁶¹Osaka City University, Osaka 558-8585
- ⁶²Pacific Northwest National Laboratory, Richland, Washington 99352
- ⁶³Panjab University, Chandigarh 160014
- ⁶⁴Peking University, Beijing 100871
- ⁶⁵University of Pittsburgh, Pittsburgh, Pennsylvania 15260
- ⁶⁶Punjab Agricultural University, Ludhiana 141004
- ⁶⁷Theoretical Research Division, Nishina Center, RIKEN, Saitama 351-0198
- ⁶⁸University of Science and Technology of China, Hefei 230026
- ⁶⁹Showa Pharmaceutical University, Tokyo 194-8543
- ⁷⁰Soongsil University, Seoul 156-743
- ⁷¹University of South Carolina, Columbia, South Carolina 29208
- ⁷²Sungkyunkwan University, Suwon 440-746
- ⁷³School of Physics, University of Sydney, New South Wales 2006
- ⁷⁴Department of Physics, Faculty of Science, University of Tabuk, Tabuk 71451
- ⁷⁵Tata Institute of Fundamental Research, Mumbai 400005
- ⁷⁶Department of Physics, Technische Universität München, 85748 Garching
- ⁷⁷Toho University, Funabashi 274-8510
- ⁷⁸Department of Physics, Tohoku University, Sendai 980-8578
- ⁷⁹Earthquake Research Institute, University of Tokyo, Tokyo 113-0032
- ⁸⁰Department of Physics, University of Tokyo, Tokyo 113-0033
- ⁸¹Tokyo Institute of Technology, Tokyo 152-8550
- ⁸²Tokyo Metropolitan University, Tokyo 192-0397
- ⁸³Virginia Polytechnic Institute and State University, Blacksburg, Virginia 24061
- ⁸⁴Wayne State University, Detroit, Michigan 48202
- ⁸⁵Yamagata University, Yamagata 990-8560
- ⁸⁶Yonsei University, Seoul 120-749



(Received 8 October 2018; published 18 January 2019)

We report a measurement of time-dependent CP violation in $B^0 \rightarrow K_S^0 \pi^0 \pi^0$ decays using a data sample of 772×10^6 $B\bar{B}$ pairs collected by the Belle experiment running at the $\Upsilon(4S)$ resonance at the KEKB e^+e^- collider. This decay proceeds mainly via a $b \rightarrow sd\bar{d}$ “penguin” amplitude. The results are $\sin 2\phi_1^{\text{eff}} = 0.92_{-0.31}^{+0.27}$ (stat.) ± 0.11 (syst.) and $\mathcal{A} = 0.28 \pm 0.21$ (stat.) ± 0.04 (syst.), which are the most precise measurements of CP violation in this decay mode to date. The value for the CP -violating parameter $\sin 2\phi_1^{\text{eff}}$ is consistent with that obtained using decay modes proceeding via a $b \rightarrow c\bar{c}s$ “tree” amplitude.

DOI: 10.1103/PhysRevD.99.011102

In the Standard Model (SM), CP violation in the quark sector is induced by a complex phase in the Cabibbo-Kobayashi-Maskawa (CKM) quark mixing matrix [1]. At $\Upsilon(4S) \rightarrow B\bar{B}$ transitions, for neutral B meson decays into a CP eigenstate produced, the decay rate has a time dependence [2,3]

$$\mathcal{P}(\Delta t, q) = \frac{e^{-|\Delta t|/\tau_{B^0}}}{4\tau_{B^0}} \times (1 + q[\mathcal{S} \sin(\Delta m_d \Delta t) + \mathcal{A} \cos(\Delta m_d \Delta t)]), \quad (1)$$

where \mathcal{S} and \mathcal{A} are CP -violating parameters; $q = 1$ for \bar{B}^0 decays and -1 for B^0 decays; Δt is the difference in decay times of the B^0 and \bar{B}^0 mesons; Δm_d is the mass difference between the two mass eigenstates of the $B^0 - \bar{B}^0$ system; and τ_{B^0} is the B^0 lifetime. As the $B^0 \rightarrow K_S^0 \pi^0 \pi^0$ decays proceed mainly via a $b \rightarrow sd\bar{d}$ “penguin” amplitude, and the final state is CP even [4], the SM expectation is $\mathcal{S} \approx -\sin 2\phi_1$ and $\mathcal{A} \approx 0$, where $\phi_1 = \arg[(-V_{cd}V_{cb}^*)/(V_{td}V_{tb}^*)]$ [5]. Deviations from these expectations could indicate new physics. The value of $\sin 2\phi_1$ is well measured using decays proceeding via a $b \rightarrow c\bar{c}s$ tree amplitude, and thus comparing our measurement of $\sin 2\phi_1^{\text{eff}}$ to the $b \rightarrow c\bar{c}s$ value [6,7] provides a test of the SM [8]. We note that there is a $b \rightarrow u\bar{u}s$ tree amplitude that also contributes to $B^0 \rightarrow K_S^0 \pi^0 \pi^0$ decays and can shift ϕ_1^{eff} from ϕ_1 ; however, this amplitude is doubly Cabibbo suppressed, and thus the resulting shift is very small [9]. Previously, the BABAR experiment studied this decay and measured $\sin 2\phi_1^{\text{eff}} = -0.72 \pm 0.71 \pm 0.08$ [10]; here we present the first such measurement from the Belle experiment using a data sample 3.4 times larger than that of BABAR.

The Belle detector is a large-solid-angle magnetic spectrometer that consists of a silicon vertex detector (SVD), a 50-layer central drift chamber (CDC), an array of aerogel threshold Cherenkov counters (ACC), a barrel-like

arrangement of time-of-flight scintillation counters (TOF), and an electromagnetic calorimeter comprised of CsI(Tl) crystals (ECL) located inside a superconducting solenoid coil that provides a 1.5 T magnetic field. An iron flux-return located outside the coil is instrumented to detect K_L^0 mesons and to identify muons (KLM). The detector is described in detail elsewhere [11]. Two inner detector configurations were used. A 2.0 cm radius beampipe and a 3-layer silicon vertex detector was used for the first sample of 152×10^6 $B\bar{B}$ pairs, while a 1.5 cm radius beampipe, a 4-layer silicon detector and a small-cell inner drift chamber were used to record the remaining 620×10^6 $B\bar{B}$ pairs [12].

Due to the asymmetric energies of the e^+ and e^- beams, the $\Upsilon(4S)$ is produced with a Lorentz boost of $\beta\gamma = 0.425$ nearly parallel to the $+z$ axis, which is defined as the direction opposite the e^+ beam. Since the $B^0\bar{B}^0$ pair is almost at rest in the $\Upsilon(4S)$ center-of-mass (CM) frame, the decay time difference Δt can be determined from the separation along z of the B^0 and \bar{B}^0 decay vertices: $\Delta t \approx (z_{CP} - z_{\text{tag}})/(\beta\gamma c)$, where z_{CP} and z_{tag} are z -coordinates of the decay positions of the B^0 decaying to the CP eigenstate and the other (tag-side), respectively. To reconstruct the decay vertices without the presence of primary charged tracks, we extrapolate the reconstructed K_S^0 momentum back to the region of the interaction point (IP) and use the IP profile in the transverse plane (perpendicular to the z axis) as a constraint. This method was used in a previous Belle analysis of $B^0 \rightarrow K_S^0 \pi^0$ decays [13] and is described in detail in Ref. [14]. Compared to $B^0 \rightarrow K_S^0 \pi^0$ decays, the K_S^0 in three-body $B^0 \rightarrow K_S^0 \pi^0 \pi^0$ decays has lower momentum and thus tends to decay closer to the IP; this results in about a 20% larger yield of K_S^0 decays to $\pi^+\pi^-$ inside the SVD volume with a correspondingly higher vertex reconstruction efficiency and greater precision in the B decay vertex position as discussed in Ref. [4].

In the determination of the event selection, Monte Carlo simulated events (MC) are used. For the signal, 1 million events for each of nonresonant, $K^*(892)^0 \pi^0$ and $f_0 K_S^0$, all of which decay into a $K_S^0 \pi^0 \pi^0$ final state, are generated using the EVTGEN [15] event generator package. These resonant states are also CP -eigenstates induced by same diagram as the nonresonant decay. Using these MC samples, all of the states are confirmed to be reconstructed and not to be affected by the selections. For the

Published by the American Physical Society under the terms of the Creative Commons Attribution 4.0 International license. Further distribution of this work must maintain attribution to the author(s) and the published article's title, journal citation, and DOI. Funded by SCOAP³.

background, a large number of $B\bar{B}$ and $q\bar{q}$ processes are simulated. Interactions of the particles in the Belle detector are reproduced using GEANT3 [16] with detector configuration information in each time period of the experiment.

Candidate K_S^0 decays are selected using multivariate analysis based on a neural network technique [17,18]. The input variables to select displaced vertices are as follows: the distance between two daughter pion tracks in the z direction, the flight distance in the x - y plane, the angle between the momentum of the $\pi^+\pi^-$ system and the K_S^0 candidate's vertex position vector with respect to the IP, and the shortest distance between the IP and daughter tracks of the K_S^0 candidate. In addition, we use the momenta of the K_S^0 and π , the angle between the K_S^0 and π , and hit information of daughters in the SVD and CDC. In this analysis we require that candidates satisfy the selection $0.480 \text{ GeV}/c^2 < M_{\pi^+\pi^-} < 0.516 \text{ GeV}/c^2$, where $M_{\pi^+\pi^-}$ is the reconstructed invariant mass of the charged pions. This range corresponds to approximately 3σ in the resolution of the mass.

Candidate $\pi^0 \rightarrow \gamma\gamma$ decays are reconstructed using photon candidates identified from ECL hits. We require that $M_{\gamma\gamma}$ satisfy $0.115 \text{ GeV}/c^2 < M_{\gamma\gamma} < 0.152 \text{ GeV}/c^2$, which corresponds to approximately 3σ in resolution. To improve the π^0 momentum resolution, we perform a mass-constrained fit to the two photons, assuming they originate from the IP.

In the case of multiple B^0 candidates in an event, we select the candidate that combines the π^0 of the smallest mass-constrained fit χ^2 value with the K_S^0 of the largest value of the neural network output variable.

To identify the decay $B^0 \rightarrow K_S^0\pi^0\pi^0$, we define two variables: the beam-constrained mass $M_{bc} \equiv \sqrt{(E_{\text{beam}}/c^2)^2 - |\vec{p}_B^{\text{CM}}/c|^2}$ and the energy difference $\Delta E \equiv E_{\text{beam}} - E_B^{\text{CM}}$, where \vec{p}_B^{CM} and E_B^{CM} are the B momentum and energy, respectively, in the e^+e^- CM frame. The quantity E_{beam} is the beam energy in the CM frame. The variables M_{bc} and ΔE for signal events peak at the B^0 mass and at zero, respectively, but have tails to lower values due to lost energy in the π^0 reconstruction.

To reject background $B\bar{B}$ decays resulting in the $K_S^0\pi^0\pi^0$ final state, we define veto regions for the reconstructed invariant masses $M_{K_S^0\pi^0}$ and $M_{\pi^0\pi^0}$. Decays $B^0 \rightarrow D^0X$ and $B^0 \rightarrow K_S^0\pi^0$ are rejected by vetoing the regions $1.77 \text{ GeV}/c^2 < M_{K_S^0\pi^0} < 1.94 \text{ GeV}/c^2$ and $M_{K_S^0\pi^0} > 4.8 \text{ GeV}/c^2$, respectively, for both π^0 candidates individually combined with the K_S^0 candidate. The veto region for $B^0 \rightarrow (c\bar{c})K_S^0$ is $2.8 \text{ GeV}/c^2 < M_{\pi^0\pi^0} < 3.6 \text{ GeV}/c^2$, where $(c\bar{c})$ is dominated by the charmonium mesons. Many of the two-body decays of the B^0 into a neutral meson and K_S^0 are CP eigenstates. Among such decay modes, $B^0 \rightarrow \eta K_S^0$ becomes background if photons are not detected with

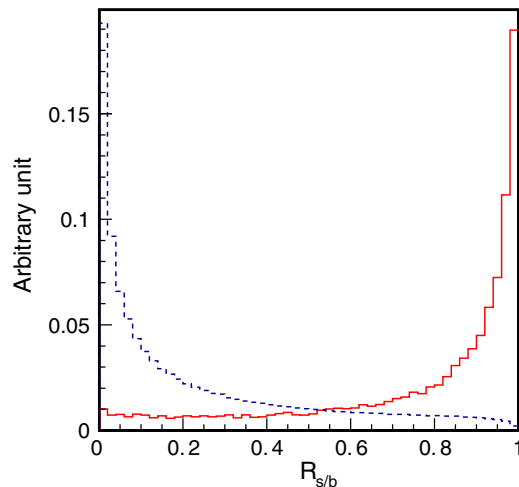


FIG. 1. Distribution of $\mathcal{R}_{s/b}$, an event-shape-based likelihood ratio, for signal and $q\bar{q}$ MC illustrated by solid and broken lines, respectively.

the decays of $\eta' \rightarrow \eta\pi^+\pi^-$, $\eta \rightarrow 2\gamma$ and $K_S^0 \rightarrow \pi^0\pi^0$ so that $M_{\pi^0\pi^0} < 0.6 \text{ GeV}/c^2$ is vetoed. In addition to those invariant masses of intermediate states, the absolute value of the cosine of the angle between the photons and the π^0 boost direction of the laboratory in the π^0 rest frame is required to be less than 0.9 to reject $B \rightarrow X_s\gamma$ decays, where X_s denotes the hadronic state governed by a radiative penguin decay.

To suppress $e^+e^- \rightarrow q\bar{q}$ continuum background events, a likelihood ratio $\mathcal{R}_{s/b}$ is calculated using modified Fox-Wolfram moments [19,20] and the cosine of the angle between the beam direction and B^0 flight direction in the CM frame, $\cos\theta_B$. Figure 1 shows the $\mathcal{R}_{s/b}$ distribution of the signal and $q\bar{q}$ MC. We impose a loose requirement $\mathcal{R}_{s/b} > 0.50$, which rejects 84% of continuum background while retaining 90% of signal decays. We subsequently include a probability density function (PDF) for $\mathcal{R}_{s/b}$ when fitting for the signal yield.

The vertex of the tag-side B is reconstructed from all charged tracks in the event, except for the K_S^0 daughters, using a vertex reconstruction algorithm described in Ref. [21]. To determine the B^0 flavor q , a multidimensional likelihood-based method for inclusive properties of particles not associated with the signal B^0 candidate is used [22]. The quality of the flavor tagging result is expressed by r , where $r = 0$ corresponds to no flavor discrimination, and $r = 1$ corresponds to unambiguous flavor assignment. Candidates with $r \leq 0.10$ are not considered further for CP violation measurement. The wrong tag fractions for six r intervals, w_l ($l = 1 - 6$), and their differences between B^0 and \bar{B}^0 decays, Δw_l , are determined from large control samples of self-tagging $B^0 \rightarrow D^{*-}\ell^+\nu$, $B^0 \rightarrow D^{(*)-}h^+(h = \pi, \rho)$ decays. The total effective tagging efficiency defined as $\Sigma(f_i \times (1 - 2w_i)^2)$ is determined to

be $(29.8 \pm 0.4)\%$, where f_l is the fraction of the events in the l th interval.

After applying all selection criteria, the signal yield is extracted from a three-dimensional unbinned maximum likelihood fit to M_{bc} , ΔE , and $\mathcal{R}_{s/b}$. For signal and $B\bar{B}$ background, the PDFs are modeled as binned histograms determined from MC simulation. A two-dimensional PDF is used for M_{bc} and ΔE , taking into account the correlation between these variables. The $q\bar{q}$ background PDF for M_{bc} is modeled by an ARGUS function [23], and that for ΔE is modeled by a second-order polynomial function. A binned histogram from the MC is used for the $q\bar{q}$ background PDF of $\mathcal{R}_{s/b}$. From the 43225 events in the regions of $M_{bc} > 5.2$ GeV/ c^2 , -0.25 GeV $< \Delta E < 0.25$ GeV, and $\mathcal{R}_{s/b} > 0.5$, the yields of signal, $q\bar{q}$ and $B\bar{B}$ are found to be 335 ± 37 , 38599 ± 262 and 4290 ± 190 , respectively. Figure 2 shows the data distribution in the signal-enhanced region $M_{bc} > 5.27$ GeV/ c^2 , -0.15 GeV $< \Delta E < 0.10$ GeV, and $\mathcal{R}_{s/b} > 0.9$, together with the fit projections, where the selection requirement on the plotted quantity is released.

To measure the CP violation parameters, an unbinned maximum likelihood fit is performed for the Δt distribution using q from the flavor tagging procedure and the signal fraction evaluated from the signal extraction fit. The PDF for the signal is set to take the form of Eq. (2) which is obtained by modifying Eq. (1) for wrong tagging and vertex resolution:

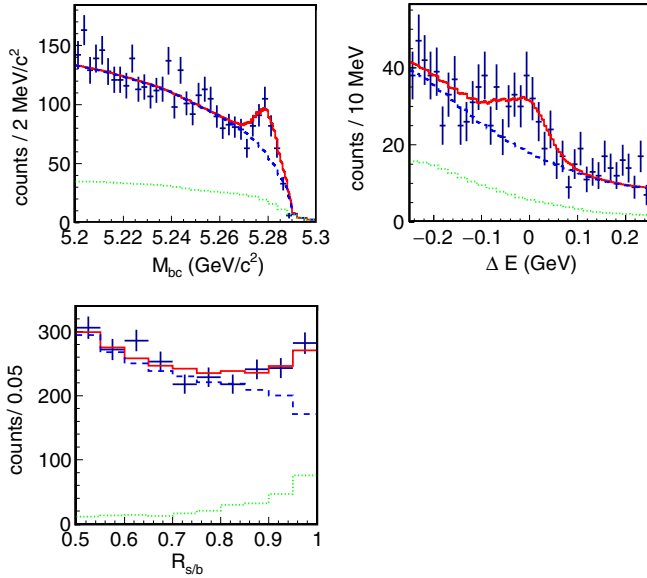


FIG. 2. M_{bc} , ΔE and $\mathcal{R}_{s/b}$ distributions (points with uncertainties) using signal-enhanced selections $M_{bc} > 5.27$ GeV/ c^2 , -0.15 GeV $< \Delta E < 0.10$ GeV, and $\mathcal{R}_{s/b} > 0.9$ except for the variable displayed. The fit result is illustrated by the solid curve, while the total and $B\bar{B}$ backgrounds are shown by broken and dotted curves, respectively.

$$\mathcal{P}(\Delta t, q) = \frac{e^{-|\Delta t|/\tau_{B^0}}}{4\tau_{B^0}} (1 - q\Delta w + (1 - 2w)q[\mathcal{S} \sin(\Delta m_d \Delta t) + \mathcal{A} \cos(\Delta m_d \Delta t)]) \otimes R(\Delta t). \quad (2)$$

Here $R(\Delta t)$ is a convolved resolution function consisting of three components: the detector resolution for z_{CP} and z_{tag} vertices, the shift of z_{tag} due to secondary tracks, and the kinematic approximation used in calculating Δt from the vertex positions. These are determined using a large CP -conserving sample of semileptonic and hadronic B decays. For the background, which includes both $q\bar{q}$ and $B\bar{B}$, the PDF is modeled as a combination of two Gaussian functions and a delta function, as determined from the sideband regions 5.20 GeV/ $c^2 < M_{bc} < 5.26$ GeV/ c^2 , -1.00 GeV $< \Delta E < -0.40$ GeV and 0.20 GeV $< \Delta E < 0.50$ GeV. τ_B and Δm_d are fixed to world average values [24]. For the resolution function $R(\Delta t)$, a broad Gaussian function is included to account for a small outlier component. The number of events within the three-dimensional region of $M_{bc} > 5.27$ GeV/ c^2 , -0.15 GeV $< \Delta E < 0.10$ GeV and $\mathcal{R}_{s/b} > 0.5$ with vertices and flavor information is 964, and the purity is 11.4%. From fitting these events we obtain $\mathcal{S} = -0.92^{+0.31}_{-0.27}$ and $\mathcal{A} = 0.28 \pm 0.21$, where the errors are statistical only. Figure 3 shows the Δt distribution of each flavor together with the background.

The systematic uncertainties are summarized in Table I. Systematic uncertainties originating from vertexing opposite the CP side, flavor tagging, and fixed physics parameters, and tag-side interference [25] are estimated from studying the large statistic data sample of the $B^0 \rightarrow (c\bar{c})K^0$

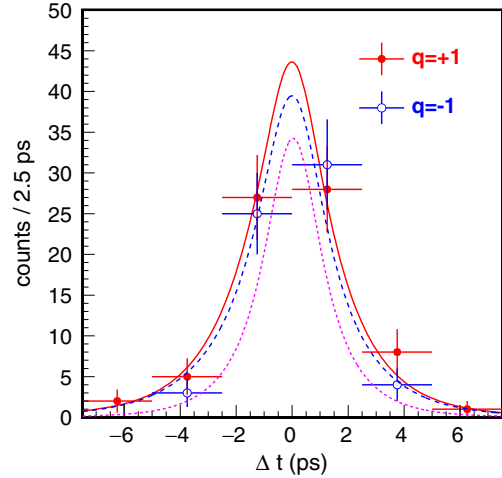


FIG. 3. Δt distribution shown by data points with uncertainties, and fit result with curves: filled circles with error bars along with a solid-line fit curve correspond to $q = +1$, while open circles with error bars along with a dashed-line fit curve correspond to $q = -1$. The background contribution is illustrated by the dotted line. Events with good flavor tagging quality ($r > 0.5$) are shown.

TABLE I. Systematic uncertainties.

	$\Delta \sin 2\phi_1^{\text{eff}}$	$\Delta \mathcal{A}$
Vertexing	± 0.02	± 0.01
Flavor tagging	± 0.004	± 0.003
Resolution function	± 0.06	$^{+0.004}_{-0.003}$
Physics parameters	± 0.002	< 0.001
Fit bias	± 0.03	± 0.02
Background fraction	± 0.02	± 0.02
Background Δt	± 0.08	± 0.02
Tag-side interference	± 0.001	± 0.008
Total	± 0.11	± 0.04

analysis [6]. Uncertainty from vertex reconstruction using K_S^0 including the resolution function is estimated using a large control sample of $B^0 \rightarrow J/\psi K_S^0$ decays. Fit bias is estimated by fitting a large number of signal MC samples and evaluating the resulting deviation compared to the input. For the PDF shape, the uncertainty is estimated using a smeared distribution. For parameters fixed in the fit, such as the signal fraction and background Δt PDF, the uncertainties are estimated by shifting these parameters by their errors and refitting; the resulting changes in \mathcal{S} and \mathcal{A} are taken as the systematic uncertainties. Including the systematic uncertainty, we determine that $\sin 2\phi_1^{\text{eff}} = 0.92_{-0.31}^{+0.27} \pm 0.11$ and $\mathcal{A} = 0.28 \pm 0.21 \pm 0.04$, where the first and second errors are statistic and systematic, respectively.

In summary, we measure CP violation parameters in the decay $B^0 \rightarrow K_S^0 \pi^0 \pi^0$ using $772 \times 10^6 B\bar{B}$ pairs and obtain

$$\begin{aligned} \mathcal{S} &= -0.92_{-0.27}^{+0.31}(\text{stat}) \pm 0.11(\text{syst}), \\ \mathcal{A} &= 0.28 \pm 0.21(\text{stat}) \pm 0.04(\text{syst}). \end{aligned}$$

The result for \mathcal{S} is consistent with the value measured from decays mediated by a $b \rightarrow c\bar{c}s$ transition, $\sin 2\phi_1 = 0.698 \pm 0.017$ [26]. The result for \mathcal{A} is consistent with zero, i.e., no direct CP violation, as expected in the SM. This is the first result obtained by the Belle experiment for this mode (and it is the third CP -even eigenstate from $b \rightarrow sq\bar{q}$ transitions used by Belle for the $\sin 2\phi_1^{\text{eff}}$ measurement after $B^0 \rightarrow \eta' K_L^0$ and $B^0 \rightarrow \phi K_L^0$).

We thank the KEKB group for the excellent operation of the accelerator; the KEK cryogenics group for the

efficient operation of the solenoid; and the KEK computer group, the National Institute of Informatics, and the Pacific Northwest National Laboratory (PNNL) Environmental Molecular Sciences Laboratory (EMSL) computing group for valuable computing and Science Information NETwork 5 (SINET5) network support. We acknowledge support from the Ministry of Education, Culture, Sports, Science, and Technology (MEXT) of Japan, the Japan Society for the Promotion of Science (JSPS), and the Tau-Lepton Physics Research Center of Nagoya University; the Australian Research Council; Austrian Science Fund under Grant No. P 26794-N20; the National Natural Science Foundation of China under Contracts No. 11435013, No. 11475187, No. 11521505, No. 11575017, No. 11675166, and No. 11705209; Key Research Program of Frontier Sciences, Chinese Academy of Sciences (CAS), Grant No. QYZDJ-SSW-SLH011; the CAS Center for Excellence in Particle Physics (CCEPP); Fudan University Grants No. JIH5913023, No. IDH5913011/003, No. JIH5913024, and No. IDH5913011/002; the Ministry of Education, Youth and Sports of the Czech Republic under Contract No. LTT17020; the Carl Zeiss Foundation, the Deutsche Forschungsgemeinschaft, the Excellence Cluster Universe, and the VolkswagenStiftung; the Department of Science and Technology of India; the Istituto Nazionale di Fisica Nucleare of Italy; National Research Foundation (NRF) of Korea Grants No. 2014R1A2A2A01005286, No. 2015R1A2A2A01003280, No. 2015H1A2A1033649, No. 2016R1D1A1B01010135, No. 2016K1A3A7A09005 603, and No. 2016R1D1A1B02012900; Radiation Science Research Institute, Foreign Large-size Research Facility Application Supporting project and the Global Science Experimental Data Hub Center of the Korea Institute of Science and Technology Information; the Polish Ministry of Science and Higher Education and the National Science Center; the Ministry of Education and Science of the Russian Federation and the Russian Foundation for Basic Research; the Slovenian Research Agency; Ikerbasque, Basque Foundation for Science, Basque Government (No. IT956-16) and Ministry of Economy and Competitiveness (MINECO) (Juan de la Cierva), Spain; the Swiss National Science Foundation; the Ministry of Education and the Ministry of Science and Technology of Taiwan; and the United States Department of Energy and the National Science Foundation.

- [1] M. Kobayashi and T. Maskawa, *Prog. Theor. Phys.* **49**, 652 (1973).
- [2] A. B. Carter and A. I. Sanda, *Phys. Rev. Lett.* **45**, 952 (1980); *Phys. Rev. D* **23**, 1567 (1981); I. I. Bigi and A. I. Sanda, *Nucl. Phys.* **193**, 85 (1981).
- [3] A general review of the formalism is given in I. I. Bigi, V. A. Khoze, N. G. Uraltsev, and A. I. Sanda, *CP Violation*, edited by C. Jarlskog (World Scientific, Singapore, 1989), p. 175.
- [4] T. Gershon and M. Hazumi, *Phys. Lett. B* **596**, 163 (2004).
- [5] Another naming convention, $\beta(=\phi_1)$, is also used in the literature.
- [6] I. Adachi *et al.* (Belle Collaboration), *Phys. Rev. Lett.* **108**, 171802 (2012).
- [7] B. Aubert *et al.* (BABAR Collaboration), *Phys. Rev. D* **79**, 072009 (2009).
- [8] Y. Grossman and M. Woarh, *Phys. Lett. B* **395**, 241 (1997).
- [9] H.-Y. Cheng, [arXiv:hep-ph/0702252](https://arxiv.org/abs/hep-ph/0702252).
- [10] B. Aubert *et al.* (BABAR Collaboration), *Phys. Rev. D* **76**, 071101 (2007).
- [11] A. Abashian *et al.* (Belle Collaboration), *Nucl. Instrum. Methods Phys. Res., Sect. A* **479**, 117 (2002); also see detector section in J. Brodzicka *et al.*, *Prog. Theor. Exp. Phys.* **2012**, 04D001 (2012).
- [12] Z. Natkaniec *et al.* (Belle SVD2 Group), *Nucl. Instrum. Methods Phys. Res., Sect. A* **560**, 1 (2006).
- [13] M. Fujikawa *et al.* (Belle Collaboration), *Phys. Rev. D* **81**, 011101 (2010).
- [14] K. Sumisawa *et al.* (Belle Collaboration), *Phys. Rev. Lett.* **95**, 061801 (2005).
- [15] D. J. Lange, *Nucl. Instrum. Methods Phys. Res., Sect. A* **462**, 152 (2001).
- [16] R. Brun *et al.*, Report No. CERN DD/EE/84-1, 1984.
- [17] M. Feindt and U. Kerzel, *Nucl. Instrum. Methods Phys. Res., Sect. A* **559**, 190 (2006).
- [18] H. Nakano, Ph. D. thesis, Tohoku University, 2014, Ch. 4 (unpublished), https://tohoku.repo.nii.ac.jp/?action=pages_view_main&active_action=repository_view_main_item_detail&item_id=70563&item_no=1&page_id=33&block_id=38.
- [19] The Fox-Wolfram moments were introduced in G. C. Fox and S. Wolfram, *Phys. Rev. Lett.* **41**, 1581 (1978); The Fisher discriminant used by Belle, based on modified Fox-Wolfram moments (SFW), is described in K. Abe *et al.* (Belle Collaboration), *Phys. Rev. Lett.* **87**, 101801 (2001); K. Abe *et al.* (Belle Collaboration), *Phys. Lett. B* **511**, 151 (2001).
- [20] S. H. Lee *et al.* (Belle Collaboration), *Phys. Rev. Lett.* **91**, 261801 (2003).
- [21] H. Tajima *et al.*, *Nucl. Instrum. Methods Phys. Res., Sect. A* **533**, 370 (2004).
- [22] H. Kakuno *et al.*, *Nucl. Instrum. Methods Phys. Res., Sect. A* **533**, 516 (2004).
- [23] H. Albrecht *et al.* (ARGUS Collaboration), *Phys. Lett. B* **241**, 278 (1990).
- [24] M. Tanabashi *et al.* (Particle Data Group), *Phys. Rev. D* **98**, 030001 (2018).
- [25] O. Long, M. Baak, R. N. Cahn, and D. Kirkby, *Phys. Rev. D* **68**, 034010 (2003).
- [26] Y. Amhis *et al.* (Heavy Flavor Averaging Group), *Eur. Phys. J. C* **77**, 895 (2017).